

doi:10.15199/48.2023.03.12

Correlation method of compensating the zero temperature-drift of four-electrode low-range electrochemical NO₂ and SO₂ gas concentration sensors

Abstract. In the paper was presented a method of compensating for the temperature drift of the zero component of four-electrode low-range electrochemical sensors of gas concentration: nitrogen dioxide and sulfur dioxide. The method is based on a long-term series of measurement results from these sensors. Statistical analysis of the results at changing ambient temperature enables the identification of temperature drift baseline that is unique for a given sensor unit. The accuracy of the curve estimation was additionally increased by using a series of results from standard measures in the validation process. The proposed method is to facilitate the use of electrochemical sensors for the construction of cheap and portable detectors of nitrogen dioxide and sulfur dioxide concentrations included in the atmospheric air.

Streszczenie. W pracy przedstawiono metodę kompensacji dryftu temperaturowego składowej zerowej czteroelektrodowych niskozakresowych elektrochemicznych sensorów stężenia gazów: dwutlenku azotu i dwutlenku siarki. Metoda opiera się na długiej serii wyników pomiarów z tych czujników. Analiza statystyczna wyników przy zmieniającej się temperaturze otoczenia umożliwia identyfikację krzywej bazowej dryftu temperatury, która jest unikalna dla danego egzemplarza sensora. Dokładność estymacji krzywej została dodatkowo zwiększona poprzez wykorzystanie w procesie walidacji serii wyników kryterium minimalizacji odchylenia standardowego. Proponowana metoda może ułatwić wykorzystanie sensorów elektrochemicznych do budowy tanich i przenośnych detektorów stężeń dwutlenku azotu i dwutlenku siarki zawartych w powietrzu atmosferycznym. (**Korelacyjna metoda kompensacji zerowego dryftu temperaturowego czteroelektrodowych elektrochemicznych czujników niskiego zakresu stężenia gazów NO₂ i SO₂**)

Keywords: four-electrode electrochemical sensor; low-range NO₂ and SO₂ sensors; temperature-dependent baseline effects, temperature-drift compensation.

Słowa kluczowe: czteroelektrodowy sensor elektrochemiczny; niskozakresowe sensory NO₂ i SO₂; krzywa bazowa zależna od temperatury, kompensacja dryftu temperatury.

Introduction

The adverse health effects of airborne gases such as nitrogen dioxide (NO₂) and sulfur dioxide (SO₂) are well documented. Under Directive 2008/50 / EC of the European Union (EU) on air quality, Member States are required to monitor air quality in areas where it is expected that the permissible limits may be exceeded. In Poland, the national network of air pollution measurement stations is operated by the Chief Inspectorate for Environmental Protection (CIEP – GIOŚ in Polish). The permissible levels of NO₂ and SO₂ content in the air considered safe are: 40 µg/m³ and 50 µg/m³, respectively, and after conversion to the relative number of particles the limits are at the level of several to several tens parts per billion: 20.92 and 18.79 ppb. Measurement of such low gas concentrations requires the use of low-range sensors as well as precise measurement amplifiers characterized by a unique stability of parameters.

Gas concentration meters used in measuring stations of GIOŚ are based on precise but expensive techniques, mainly chemiluminescent or dispersion techniques. In order to densify the monitoring network, the use of much cheaper amperometric electrochemical sensors has been considered for a long time, the small size of which is an additional advantage enabling the construction of cheap portable measuring devices. The disadvantage of electrochemical sensors, which hinders their widespread implementation, is the high susceptibility of the measurement result to temperature and humidity changes. Temperature strongly influences the sensitivity and the zero component, that is the response to clean air. Sensitivity temperature drift due to the small production spread can be easily compensated for by a rigid, typical correction relationship given by the manufacturer. The compensation of the temperature drift of zero is, however, a greater challenge, due to the high values and large spread in individual units. Additionally, a long-term aging effect of the sensitivity decrease, and the zero changes is observed. The effect of humidity on the response usually becomes

apparent with rapid deep changes. Especially rapid large drops are accompanied by long-term severe disturbance of the response.

This paper is devoted to the zero drift compensation of electrochemical sensors used in a portable air quality detector (Fig. 1), which is being developed by a team of designers at Emag-Serwis sp. z o.o., as part of the project financed by National Centre of Research and Development, Poland, within the framework of the Smart Growth Operational Programme, POIR.04.01.04-00-0060/19.



Fig. 1. The portable air quality detector created in the project

Problems with determining the zero drift

The first step was to measure the zero as a function of temperature, in laboratory conditions in a climatic chamber, by supplying clean air from a reference cylinder.

Unfortunately, the clean air cylinders available in the offer contain pollutants, including NO₂ and SO₂, at the level of several to several tens ppb. As a result, a response was obtained not only to the temperature change, but also to the unknown, but significant, concentration of the measured gas. In addition, the air supplied from the cylinder has a

very low humidity, below 20%, which causes the electrolyte to dry out, which resulted in an additional change in the responses of the sensors. An attempt was also made to calibrate the sensors zero by giving a standard sample with a known gas concentration. For this purpose, reference gas cylinders with different concentrations were used, e.g., 800 ppb, 2,000 ppb and a clean air cylinder, and the research laboratory was equipped with a precise gas mixer Sonimix 7100 Gas Divider of the LNI Swissgas SA. Unfortunately, in this case the problem of gas consumption by the elements of the gas supply and mixing path (hoses, valves, reducers, mixer) was encountered, as a result of which a sample with a significantly lower value reached the sensor (Fig. 2).

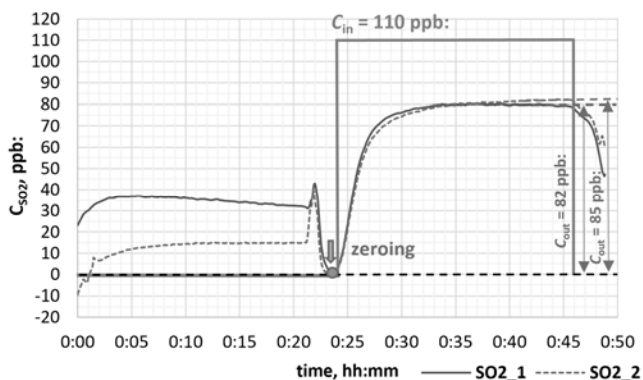


Fig. 2. Reduced response C_{out} of two exemplary SO₂ sensors to the supply of a gas sample with a concentration of $C_{in} = 110$ ppb

The aim of this work is to analyze the possibility of compensation of the zero-component temperature drift by the correlation method, which consists in extracting the base curve of this drift by finding the correlation between temperature and sensor response, based on a long-term data series of results with high time resolution. The method was described in [1], [2], [3], which presented promising results of the application of the correlation methodology to compensate for the impact of changes in selected environmental parameters for the three-electrode electrochemical sensors CO and NO.

Four-electrode concentration sensors of SO₂, NO₂

As a result of many months of preliminary work, which practically analyzed the metrological properties of cheap low-range electrochemical sensors of NO₂ and SO₂ concentration, available from leading manufacturers (Winsen, SPEC Sensors, Membrapor and Alphasense), two four-electrode sensors from the Alphasense's offer were finally selected for the next stage of the project:

- sensor NO₂: NO₂-B43F [6],
- sensor SO₂: SO₂-B4 [7].

Graphic electrical symbol and dimensions of NO₂-B43F and SO₂-B4 sensors were showed on Fig. 3.

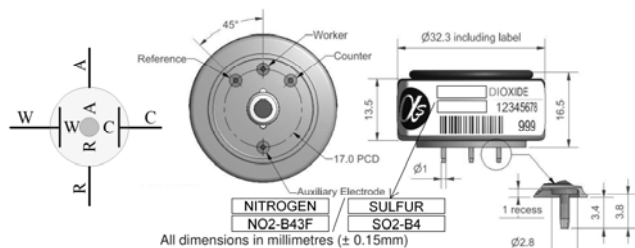


Fig. 3. Graphic electrical symbol and dimensions of NO₂-B43F [6] and SO₂-B4 [7] sensors

Selected Alphasense amperometric electrochemical gas sensors use three standard electrodes [10]:

- working electrode (W) reacts with the target gas to generate a current I_W , which is proportional to the gas concentration,
- counter electrode (C) supplies a current I_C that balances that generated by the working electrode current I_W ,
- reference electrode (R) sets the operating potential of the working electrode.

The additional fourth electrode, called the auxiliary electrode (A), has no contact with the measured gas, is similar in structure and location to the W electrode, so the current I_A generated by this electrode contains only a component dependent on environmental parameters, including temperature. Unfortunately, this component only partially coincides with the component present on the W electrode, so it cannot be compensated by simply subtracting the current I_A from I_W .

Selected parameters of sensors NO₂-B43F and SO₂-B4 were collected in table 1.

Table 1. Chosen parameters of sensors NO₂-B43F and SO₂-B4

Parameter	NO ₂ -B43F	SO ₂ -B4
Sensitivity, nA/ppb:	-0,200 ... -0,650	+0,275 ... +0,520
Range, ppb:	20 000	100 000
Noise (± 1 standard deviation), ppb:	$\pm 7,5$	$\pm 2,5$
Temperature range, °C:	-30 ... 40	-30 ... 50
Humidity range, %:	15 ... 85	-15 ... +15
Sensitivity drift, % change/year:	-20 ... -40	-20 ... -40
Zero drift, ppb change/year:	0 ... +20	-20 ... +20

Alphasense for delivered sensors gives the values of sensitivity and zero for a temperature of 20 °C. The knowledge of the sensitivity makes it unnecessary to calibrate the gain of the measurement path.

Measurement circuit

To maintain a constant voltage between electrodes C and R, the sensor was connected to the potentiometric circuit [9], shown in Fig. 5.

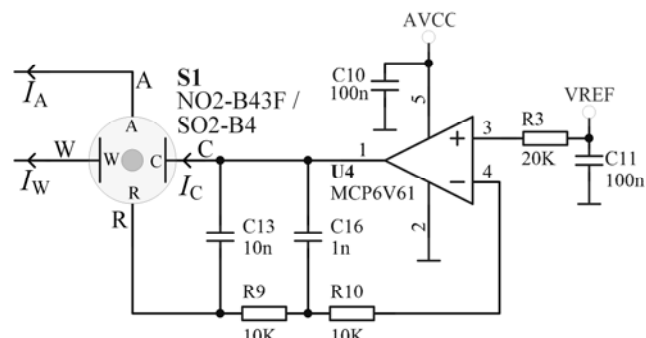


Fig. 5. Diagram of a potentiostatic circuit maintaining constant voltage between the W electrode and the R electrode of NO₂-B43F and SO₂-B4 detectors

The applied precise op amp U4: MCP6V61 meets very strict requirements:

- max input offset voltage: $\pm 100 \mu\text{V}$ – due to the permissible voltage fluctuation between electrodes C and R: $\pm 1 \text{ mV}$
- max input bias current $< 5 \text{ nA}$ – because the inverting input cannot load the C electrode with a higher current, as it would cause a disturbance of the output current I_W greater than a few ppb – after conversion to concentration.

Critical parameters values of the op amp were collected in table 2.

Table 2. Chosen parameters of sensors NO2-B43F and SO2-B4

Parameter	Value
max input offset voltage:	$\pm 8 \mu\text{V}$
max input bias current:	$\pm 50 \text{ pA}$

The connecting of the working and auxiliary electrodes to the reference electrode with the power off is ensured by the circuit with the p channel FET transistor shown in Fig. 3a. The currents I_W and I_A are measured in two identical measuring circuits with a single-stage op amp in the transimpedance configuration shown in Fig. 3b.

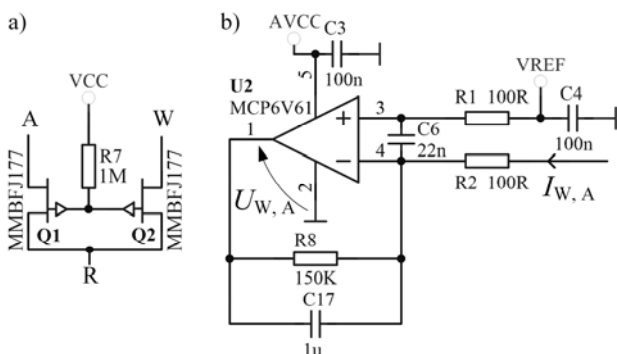


Fig. 6. Circuit diagram: a) in power off conditions short circuit of A, W electrodes with R electrode using the p channel FET transistor; b) transimpedance measuring amplifier

The amplifier transresistance R_{amp} , set by the resistance of the resistor R8, is 0.15 mV/nA . For example, assuming the gain of the sensors near the middle of the guaranteed range: -0.4 nA/ppb for NO2-B43F and $+0.4 \text{ nA/ppb}$ for SO2-B4, a concentration change by $\pm 1 \text{ ppb}$ corresponds to a change in the U_W and U_A output voltage, by $\pm 60 \mu\text{V}$. The values of the output currents I_W and I_A , after processing in separate ADC channels, are transferred to the local microcontroller, in which the temperature correction of the results can be implemented.

Preliminary temperature compensation of the zero background current

Preliminary temperature zero compensation was carried out in accordance with the procedures described in the Alphasense AAN 803-05 [8] application note, correcting the electrode current values according to the following formulas:

a) for the NO2-B43F detector – using auxiliary electrode current I_A :

$$(1) U_{Wc} = (R_{amp} \cdot I_{Wu} - U_{W0e}) - n_T (R_{amp} \cdot I_{Au} - U_{A0e}),$$

b) for the SO2-B4 detector – without using auxiliary electrode current I_A :

$$(2) U_{Wc} = (R_{amp} \cdot I_{Wu} - U_{W0e}) - R_{amp} \cdot I_{W0} - R_{amp} \cdot k_T'',$$

where: I_{Wu} – uncorrected raw value of I_W , nA, I_{Au} – uncorrected raw value of I_A , nA, U_{Wc} – corrected W output signal, mV, U_{W0e} – electronic output offset of W signal measurement channel, mV, U_{A0e} – electronic output offset of A signal measurement channel, mV, I_{W0} – the value of I_W in zero air at a temperature of 20°C , I_{A0} – the value of I_A in zero air at a temperature of 20°C .

The values of the n_T and k_T'' factors were made dependent on the temperature using linear segmental interpolation for the points collected in Table 3 – taken from Table 3 of the application note [8].

Table 3. Zero background current temperature compensation factors

Factors	Temperature, $^\circ\text{C}$								
	-30	-20	-20	0	10	20	30	40	50
$n_T, 1/^\circ\text{C}$:	1.3	1.3	1.3	1.3	1.0	0.6	0.4	0.2	-1.5
$k_T'', \text{ nA}/^\circ\text{C}$:	-4	-4	-4	-4	-4	0	20	140	450

Preparation of a long series of measurement results from sensors

The method of compensating the zero component temperature drift is based on a long series of measurement results from sensors with high time resolution. Therefore, for the purposes of the development and validation of the method, the measurement set was made (Fig. 6) containing 10 modules with NO2-B43F and SO2-B4 sensors, enabling the measurement results to be read from the sensors every 1 s.



Fig. 7. The measurement set containing 10 modules with sensors NO2- B43F and SO2-B4

In the period from 17.03.2022 to 05.05.2022, the set was installed on the roof of the local air quality measurement GIOŚ station, located in Katowice, at St. Kossutha 6 (Fig. 7).



Fig. 8. The measuring set installed on the roof of the local air quality measurement GIOŚ station (Katowice, St. Kossutha 6)

The 1-hour average values of NO₂ and SO₂ mass concentrations, expressed in $\mu\text{g}/\text{m}^3$, provided by the station, were converted into the relative number of particles expressed in ppb. Sensor results were averaged every 5 min and expressed in ppb. Then, for each sensor, the

smallest negative value was searched and with a plus sign as N_x , S_x (N - NO₂ sensor, S - SO₂ sensor, x - sensor number) was added to the raw results, thus obtaining a data series of non-negative 5-minute mean values of the measurement result.

Estimation of the overall relationship between sensor output values and temperature

In the first step, taking into account all the collected sensor data, the overall effect of temperature on the sensor responses was estimated using an approximating function optimally fitted to the series of results. The coefficient of determination R^2 was used as a measure of fit. The fit results for two units of the NO₂-B43F sensors is shown in Fig. 8 and the SO₂-B4 sensors in Fig. 9.

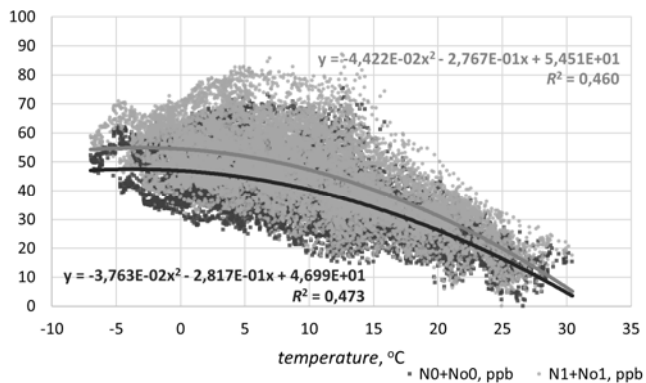


Fig. 9. The scatter of the response values of two sensors NO₂-B43F (the N0 and N1 samples) depending on the ambient temperature, recorded in the period from 17.03.2022 to 05.05.2022

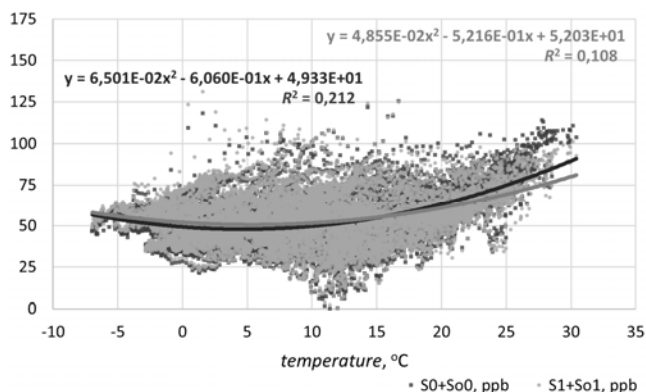


Fig. 10. The scatter of the response values of two sensors SO₂-B4 (the S0 and S1 samples) depending on the ambient temperature, recorded in the period from 17.03.2022 to 05.05.2022

The relationships fitted to the data series were approximated by a 2nd order polynomial. For the NO₂-B43F sensors, a better fit in the data series ($R^2 \approx 0.46$, $R^2 \approx 0.47$) was obtained than for the SO₂-B4 sensors ($R^2 \approx 0.11$, $R^2 \approx 0.21$). This may mean that the responses of the SO₂-B4 sensors are either less affected by temperature or that they are more affected by another environmental parameter, e.g. humidity. The responses of NO₂-B43F sensors show a decreasing trend as a function of temperature, while in the case of SO₂-B4 sensors this trend is increasing.

Extracting the baseline of the zero temperature drift

The baseline of temperature drift of the zero – this is the temperature-dependent component of the sensor's response to clean air.

Daily course of response minima

In order to extract the baseline of temperature drift of the zero, from the data series, for each subsequent day, the daily course of the response minima was first determined, which is obtained by searching for each measurement, every 5 min, the sensor's minimum response in the time window $\pm \Delta t$ (Fig. 10). The methodological assumption is that these minima are values that are statistically closest to the sensor's response to clean air at a given temperature, i.s. temperature-dependent zero of the sensor. Using the determination coefficient R^2 , the level of correlation between the course of the minima and the course of the temperature was determined for the consecutive days. As in the following days R^2 maximized at a different $\pm \Delta t$, the average of the following days was adopted for further analyzes, excluding days with low R^2 values (e.g. days with a small daily temperature amplitude). For NO₂-B43F sensors the optimal long-term interval was adopted: $\pm \Delta t = \pm 75$ min, and for SO₂-B4 sensors: $\pm \Delta t = \pm 125$ min.

Fig. 10 is a graph of several exemplary daily dependencies $R^2 = f(\Delta t)$ for the N0 instance of NO₂-B43F sensor. For SO₂-B4 sensors, significantly lower R^2 values were obtained, which indicates that the changes in zero depend less on the temperature or, apart from the temperature, another parameter (humidity) has a greater influence.

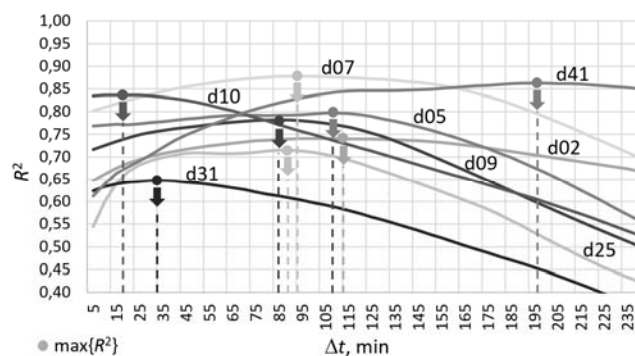


Fig. 11. Graph of several exemplary daily (d02, d05, d09, d10, d25, d31, d41) of the relationship $R^2 = f(\Delta t)$ for the NO₂-B43F sensor (the N0 sample)

An exemplary daily course of the response minima of the NO₂ sensor B43F (the N0 sample) is shown in Fig. 11, while the SO₂-B4 sensor (the S1 sample) is shown in Fig. 12.

Raw N0 sensor responses (Raw data + N0o) are positively correlated with the concentration course (REF GIOŚ data reference data) and negatively with the temperature course. The daily course of the minima of the N0 sensor response shows a negative correlation with the course of the temperature. The correlation between the raw S1 sensor response and the concentration course is not very pronounced. The humidity course has a significant but ambiguous influence. The sensor response is raised by about 25 ppb in the first part of the day when the humidity is very high, close to 100% and the temperature is positive close to zero. Next, the increase in temperature corresponds to a temporary jump in the response by another approx. 25 ppb, and when the humidity begins to rapidly drop to approx. 40%, the sensor response drops sharply by approx. 50 ppb. However, the mild increase in humidity to about 80% at the end of the day was not accompanied by any change in sensor response.

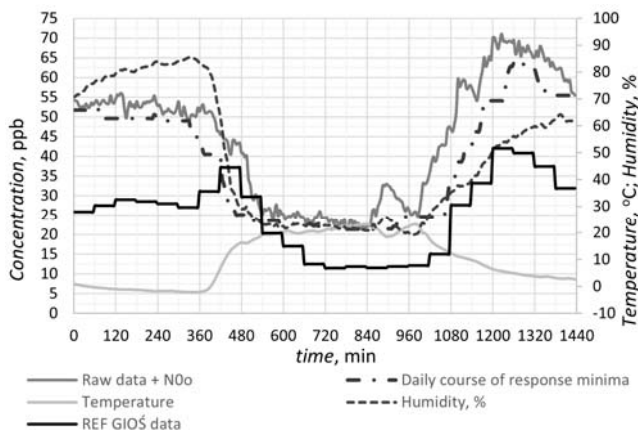


Fig. 12. An example of a daily course of response minima in the interval of $\pm\Delta t = \pm 75$ min of the NO₂-B43F sensor (the N0 sample) in the daily cycle on 25.03.2022 (d09)

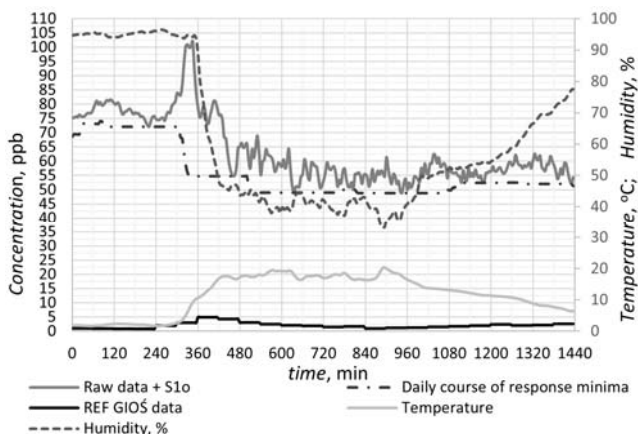


Fig. 13. An example of a daily course of response minima in the interval of $\pm\Delta t = \pm 125$ min of the SO₂-B4 sensor (the S1 sample) in the daily cycle on 27.04.2022 (d42)

Approximation fit of relationship between response minima and temperature

In the next step, for each subsequent day, the daily course of response minima was approximated with the course of temperature, using a 2nd order polynomial. Fig. 13 shows the daily scatter of the minima of the N0 sensor response as a function of temperature, on 03.05.2022, along with the determined best-fit approximation curve on a daily basis (blue curve) against the background of the final optimal curve in a long-term perspective, covering the entire study period 17.03.2022 – 05.05.2022.

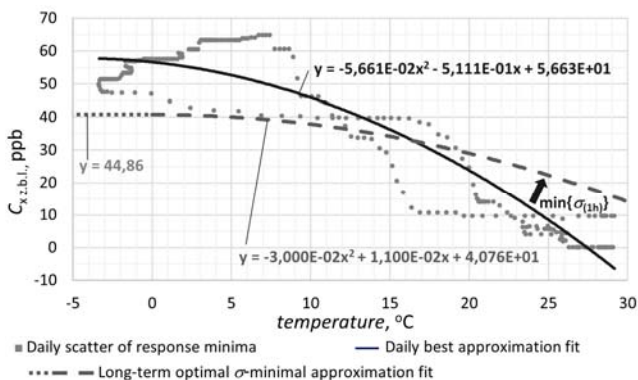


Fig. 14. Daily course of response minima in the interval of $\pm\Delta t = \pm 75$ min of the sensor NO₂-B43F (the N0 sample) in the daily cycle on 23.03.2022

Fig. 15.

Fig. 14 and Fig. 15 respectively show the long-term scatter of the sensor N0 and S1 minima as a function of

temperature. The best-fitted dependency curve drawn was approximated by a 2nd order polynomial, which, after appropriate optimization, becomes the final long-term baseline of temperature drift the zero. The polynomial approximation was limited to the range of positive temperatures, and for negative temperatures a constant term of the polynomial.

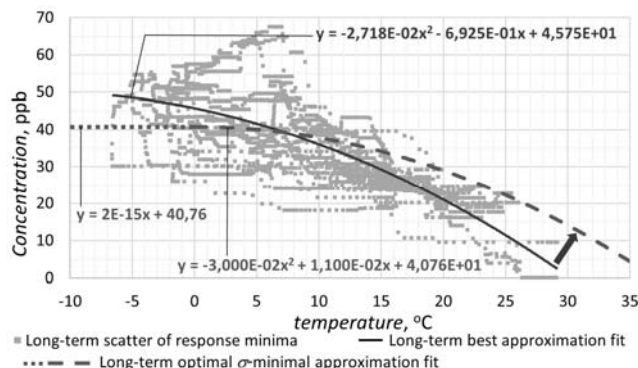


Fig. 16. Long-term course of the response minima in the interval of $\pm\Delta t = \pm 75$ min of the NO₂-B43F sensor (the N0 sample)

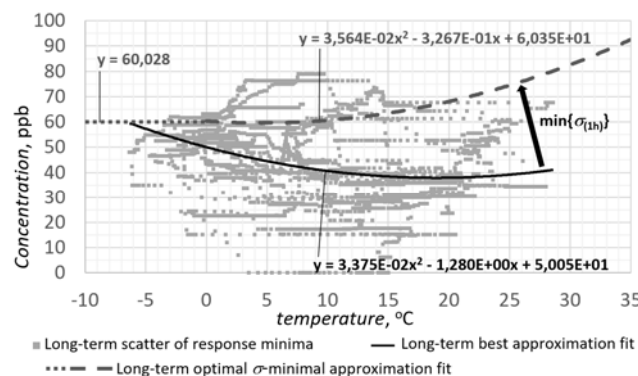


Fig. 17. Long-term course of the response minima in the interval of $\pm\Delta t = \pm 125$ min of the SO₂-B4 sensor (the S1 sample)

The coefficients of the polynomial were modified leading to the optimal case of obtaining the minimum standard deviation $\sigma_{(1h)}$ absolute error ε_i and a full long-term series of 1-hour mean values of the response:

$$(3) \quad \varepsilon_i = C_{X(1h) Det i} - C_{X(1h) REF i}$$

$C_{X(1h) Det i}$ – i -th 1-hour mean value of sensor response, $C_{X(1h) REF i}$ – i -th reference 1-hour mean value (station result). Final long-term baseline of the zero temperature drift is given by equation:

$$(4) \quad C_{X,z,b}(T) = \begin{cases} c_{z,b} & \text{for } T \leq 0^\circ\text{C} \\ a_{z,b} \cdot T^2 + b_{z,b} \cdot T + c_{z,b} & \text{for } T > 0^\circ\text{C} \end{cases}$$

The spread of the NO₂-B43F sensor response minima shows a greater focus around the long term zero drift temperature curve. In the case of the SO₂-B4 sensor, the focus is much weaker, so you can confess that entering of the temperature correction will not minimize the zero drift satisfactorily.

The correction curve of the temperature zero drift

The correction curve of temperature drift of the zero specifies a correction value to add to the raw response. It is described by the dependency:

$$(5) C_{X,z.c.}(T) = \begin{cases} c_{z.c.} & \text{for } T \leq 0^{\circ}\text{C} \\ a_{z.c.} \cdot T^2 + b_{z.c.} \cdot T + c_{z.c.} & \text{for } T > 0^{\circ}\text{C}, \end{cases}$$

where:

$$(6) \begin{aligned} a_{z.c.} &= -a_{z.b.}, & b_{z.c.} &= -b_{z.b.}, \\ c_{z.c.} &= -c_{z.b.} + C_{X(1h) \text{ Det AVG}}, \end{aligned}$$

$C_{X(1h) \text{ Det AVG}}$ – mean value of a series of 1-hour adjusted sensor response mean values.

The correction curves of temperature drift of the zero of the exemplary NO₂-B43F sensors are collected in Fig. 16 and SO₂-B4 in Fig. 17.

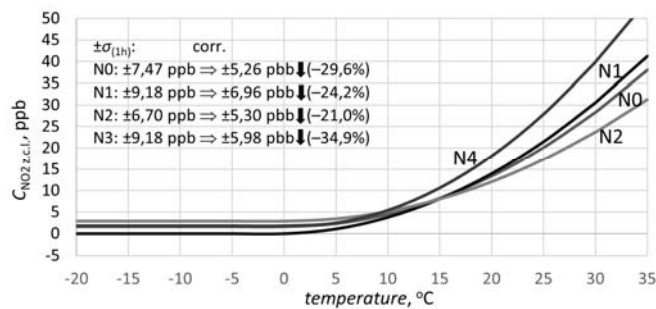


Fig. 18. The correction curves of temperature drift of the zero of the NO₂-B43F sensors (the N0, N1, N2, N3 samples)

The figures show the profit of the correction entering, expressed by a decrease in the standard deviation $\sigma_{(1h)}$ of the error of one-hourly mean values. Correction for NO₂-B43F sensors reduces the error of response (68% of results) by (21% ... 35%) to the level of $\pm\sigma_{(1h)} = \pm (5.3...7.0)$ ppb. For SO₂-B4 sensors the correction is ineffective. It causes a decrease of the response error by (9.1%... 14.3%) to the level of $\pm\sigma_{(1h)} = \pm (12.0... 12.1)$ ppb.

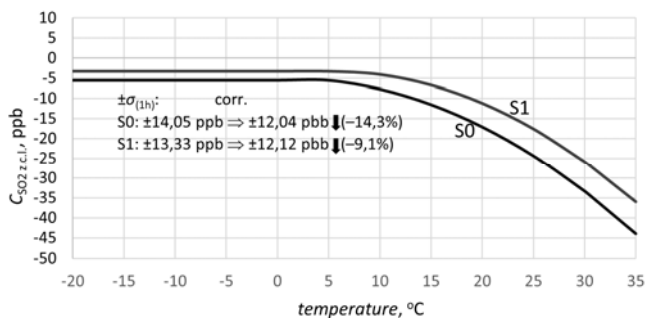


Fig. 19. The correction curves of temperature drift of the zero of the SO₂-B4 sensors (the S0 and S1 samples)

Results

An exemplary daily course of the corrected NO₂-B43F sensor responses is shown in Fig. 18 and SO₂-B4 in Fig. 19.

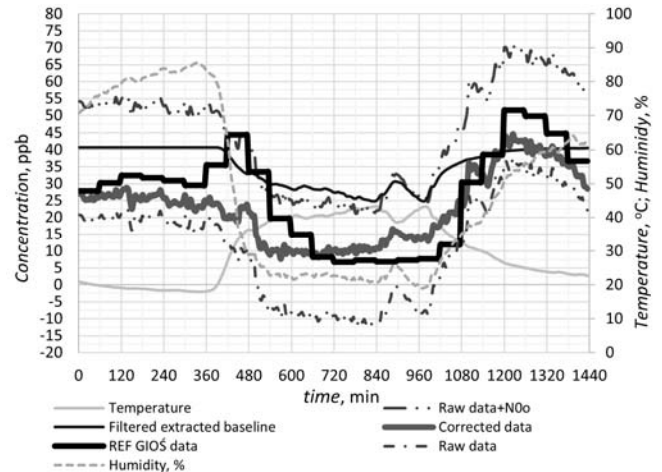


Fig. 20. An example of a daily course of the corrected responses of the NO₂-B43F sensor (the N0 sample) of 25.03.2022 (d09)

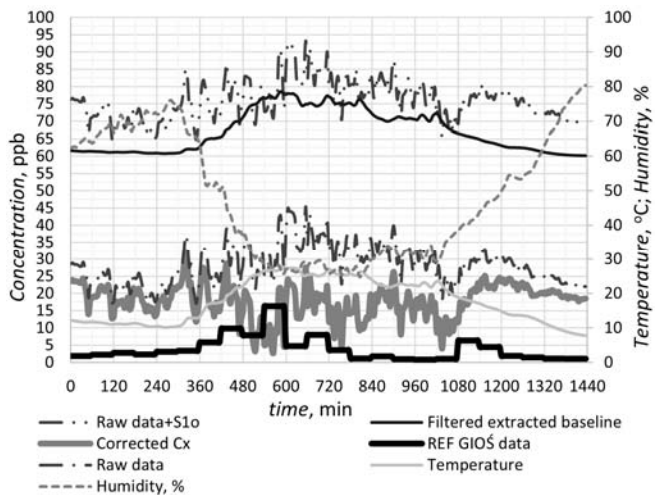


Fig. 21. An example of a daily course of the corrected responses of the SO₂-B4 sensor (the S1 sample) of 03.05.2022 (d48)

An exemplary long-term trace of the corrected 1-h average NO₂-B43F sensor responses is shown in Fig. 22, and for a selected day the diurnal course in Fig. 21. On the other hand, an exemplary of a long-term course of the corrected 1-h average responses of the SO₂-B4 sensor is shown in Fig. 22, and for a selected day, the daily course is shown in Fig. 23.

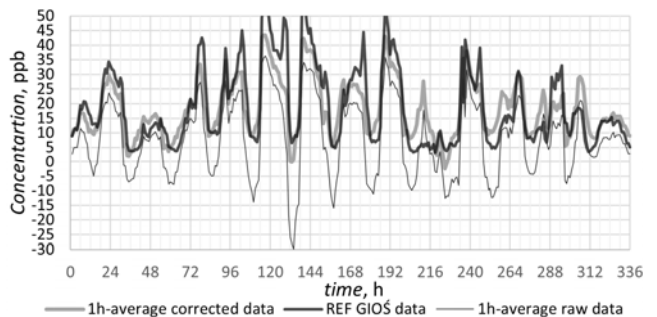


Fig. 22. An exemplary of a long-term course of the corrected 1-h average responses of the NO₂-B43F sensor (the N0 sample) over the period of 14 days, from 18.03.2022 to 31.03.2022

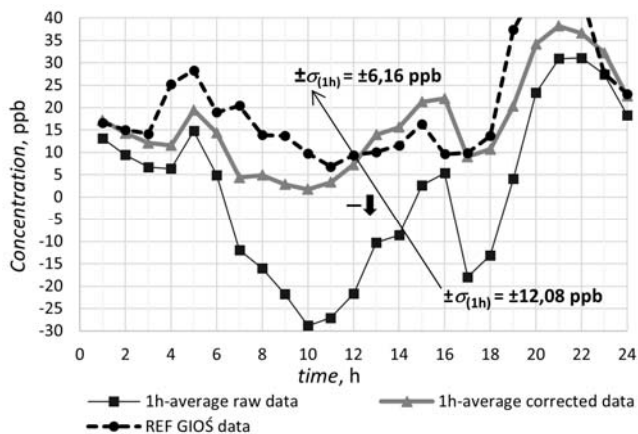


Fig. 23. An exemplary of a daily course of the corrected 1-h average responses of the NO₂-B43F sensor (the N3 sample) on 04.05.2022

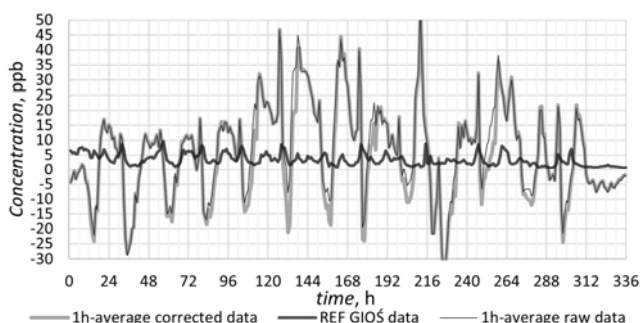


Fig. 24. An exemplary of a long-term course of the corrected 1-h average responses of the SO₂-B4 sensor (the S1 sample) over the period of 14 days, from 18.03.2022 to 31.03.2022

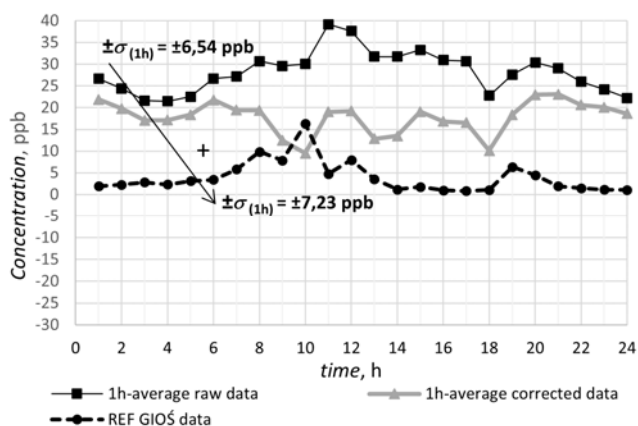


Fig. 25. An exemplary of a daily course of the corrected 1-h average responses of the SO₂-B4 sensor (the S1 sample) on 03.05.2022

Summary

The correction application of temperature drift of the zero brings positive results for the NO₂-B43F sensors. Course of the response in daily terms (Fig. 18, Fig. 21) as and long-term terms (Fig. 20), in the majority of the results coincide with the reference course with a slight error (up to ± 5 ppb). The greatest error accompanies rapid changes in

humidity and then it can reach the level of up to ± 15 ppb. After the temperature correction, NO₂-B43F sensors can be successfully used to record the NO₂ concentration, especially when limiting the presentation of results to 1-hourly averages.

In the case of SO₂-B4 sensors, the results of the temperature correction are barely visible and not sufficient to remove the zero drift. The course of the sensor response in the diurnal (Fig. 19, Fig. 23) and long-term (Fig. 22) terms do not show a noticeable correlation with the reference course. The most likely cause is the effect of humidity or cross influence other gases such O₃, which induces greater changes in sensor response than temperature. Without additional correction of the humidity influence, the SO₂-B4 sensors are not suitable for recording the SO₂ concentration in the air, because the humidity drift of the zero is several times higher than the response to the gas concentration. Therefore, in the next step, work will be undertaken to develop a method of correcting the influence of humidity on the responses of these sensors.

Author: Ph.D. Tomasz Adrikowski tomasz.adrikowski@polsl.pl, The Silesian Technical University, Department of electrical engineering and computer science, Str. Akademicka 10, 44-100 Gliwice

REFERENCES

- [1] M. I. Mead, O. A. M. Popoola, G. B. Stewart, P. Landshoff, M. Calleja, M. Hayes, J. J. Baldovi, T. Hodgson, M. McLeod, J. Dicks, A. Lewis, J. Cohen, R. Baron, J. Saffell, R. L. Jones, The use of electrochemical sensors for monitoring urban air quality in low-cost, high-density networks, *Atmospheric Environment*, vol. 70 (2013), pp. 186-203, May 2013.
- [2] O.A.M. Popoola, G. B. Stewart, M. I. Mead, R. L. Jones, Development of a baseline-temperature correction methodology for electrochemical sensors and its implications for long-term stability, *Atmospheric Environment*, vol. 147 (2016), pp. 330-343, October 2016.
- [3] E. S. Cross, L. R. Williams, D. K. Lewis, G. R. Magoon, T. B. Onasch, M. L. Kaminsky, D. R. Worsnop, J. T. Jayne, Use of electrochemical sensors for measurement of air pollution: correcting interference response and validating measurements, *Atmospheric Measurement Techniques*, vol. 10 (2017), issue 9, pp. 3575- 3588, September 2017.
- [4] J. R. Stetter, J. Li, Amperometric Gas Sensors - A Review, *Chemical Reviews* vol. 108 (2008), pp. 352-366, January 2008.
- [5] J. Li, A. Haurlyiuk, C. Malings, S. R. Eilenberg, R. Subramanian, A. A. Presto, Characterizing the Aging of Alphasense NO₂ Sensors in Long-Term Field Deployments, *ACS Sensors* vol. 6 (8), August 2021.
- [6] NO₂-B43F Nitrogen Dioxide 4-Electrode Sensor, Technical Specification, *Alphasense Ltd.*, July 2019.
- [7] SO₂-B4 Sulfur Dioxide 4-Electrode Sensor, Technical Specification, *Alphasense Ltd.*, May 2017.
- [8] AAN 803-05, Correcting for background currents in four electrode toxic gas sensors, Alphasense Application Note AAN 803-05, *Alphasense Ltd.*, June 2019.
- [9] AAN 105-03 Designing A Potentiostatic Circuit, Alphasense Application Note AAN 105-03, *Alphasense Ltd.*, March 2009.
- [10] AAN 111-02, Modelling Amperometric Electrochemical Gas Sensors, Alphasense Application Note AAN 111-02, *Alphasense Ltd.*, December 2013.